Extremely fast objects in TESS images: who they are and where they go?

András Pál

Research Centre for Astronomy and Earth Sciences, Konkoly Observatory – Budapest, Hungary

E-mail contact address: `apal@konkoly.hu, apal@szofi.hu`.

Abstract

Mainly, TESS observes an average minor planet with a quite decent apparent proper motion around a pixel or a fraction of a pixel per long cadence. However, some of the full frame images exhibit extraordinary long streaks corresponding to nearby objects with an apparent speed in the order of several minutes of arc per minute. Therefore, the parent objects of these streaks are usually visible only for a few frames. On the other hand, thanks to the on-board cosmic ray mitigation (CMR) algorithm employed by the image acquisition electronics, these streaks are chopped into smaller segments, allowing us to determine its properties within a cadence of 20 seconds.

All in all, we can say that despite the comparatively small number of frames, hundreds of individual data points are available for further analysis - allowing us to determine their physical characteristics and orbit. In this poster we exhibit few such objects and we try to answer the implied questions: who they are and where they go? Are these natural objects or artificial ones? Are these previously known or unknown ones?

TESS and the Solar System

While the primary mission of TESS has been designed to observe the Southern and Northern Ecliptic Hemispheres, avoiding the ecliptic by ~ 6 degrees, the scale height of the debris disk of our Solar System allows us to detect many prominent moving objects in the field-of-view of the spacecraft cameras. See e.g. [1], [2] or [3] for an introduction to the field. In addition to the analysis of known objects (see again [2] or [3]), TESS cameras found to be providing an interesting way of discovering objects (see e.g. [4] and [5] for various minor body families). The photometric precision of TESS instrumentation can well be predicted and found to be close to the expectations, especially when we compare to Kepler/K2 (see [6]), the previous mission providing extraordinary quality of space-borne photometry of Solar System bodies (see for example [7] and further papers in this series of articles).

Characteristics of moving objects

Basically, an average minor planet has a slow apparent motion due to the cancellation effect of the long exposure time by the comparatively large pixel size: the rule of thumb is to be in the order of a pixel per frame (see [1]). Therefore, any object moving faster than a few pixels per cadence can be considered interesting and imply a rather close approach to the observer (i.e. TESS, and not even Earth in our case). Namely, objects having an apparent speed in the order of 1000 pixels/frame are extremely close: such a speed would imply a distance of $\sim 18,000\,\mathrm{km}$ expecting a relative tangential speed of $1\,\mathrm{km/s}$ – and proportionately larger for larger speeds. Therefore, such objects can easily be inside the Earth-Moon system and can potentially be hazardous.

Cosmic ray mitigation

One of the most interesting features of TESS imaging is the implementation of the cosmic ray mitigation. Here, 10 frames of the elementary 2-second long CCD readouts are stacked by averaging the intermediate 8 values of the individual pixel values (i.e. rejecting the highest and lowest values, see [8] for more details). Longer exposures, including the short cadence stamps of 2 minutes and the full-frame images of 30 minutes (or 10 minutes) are the sums of 6, 90 (or 30) of these 20-second long elementary readouts.

This algorithm efficiently removes the cosmic ray hits, however, streaks corresponding to fast moving objects are going to be chopped in accordance to the 20-second long units of readout. This is also prominent in the so-called firefly effect (see [9]) which is caused by the dust particles leaving the spacecraft. However, such chopping helps us to easily treat these long streaks as a series of individual data points – and therefore obtain a very fine sampling cadence even using purely full-frame images.

An example object on one of the S9/Cam1/CCD3 images

In the following, we analyze the *sole* FFI frame taken during Sector 9 observations, at the cadence of `2019071195934`. By analyzing this frame, it is shown here that photometric and astrometric analysis is feasible at the time resolution of 20 seconds – by employing the side-effects of the on-board cosmic ray mitigation of TESS.

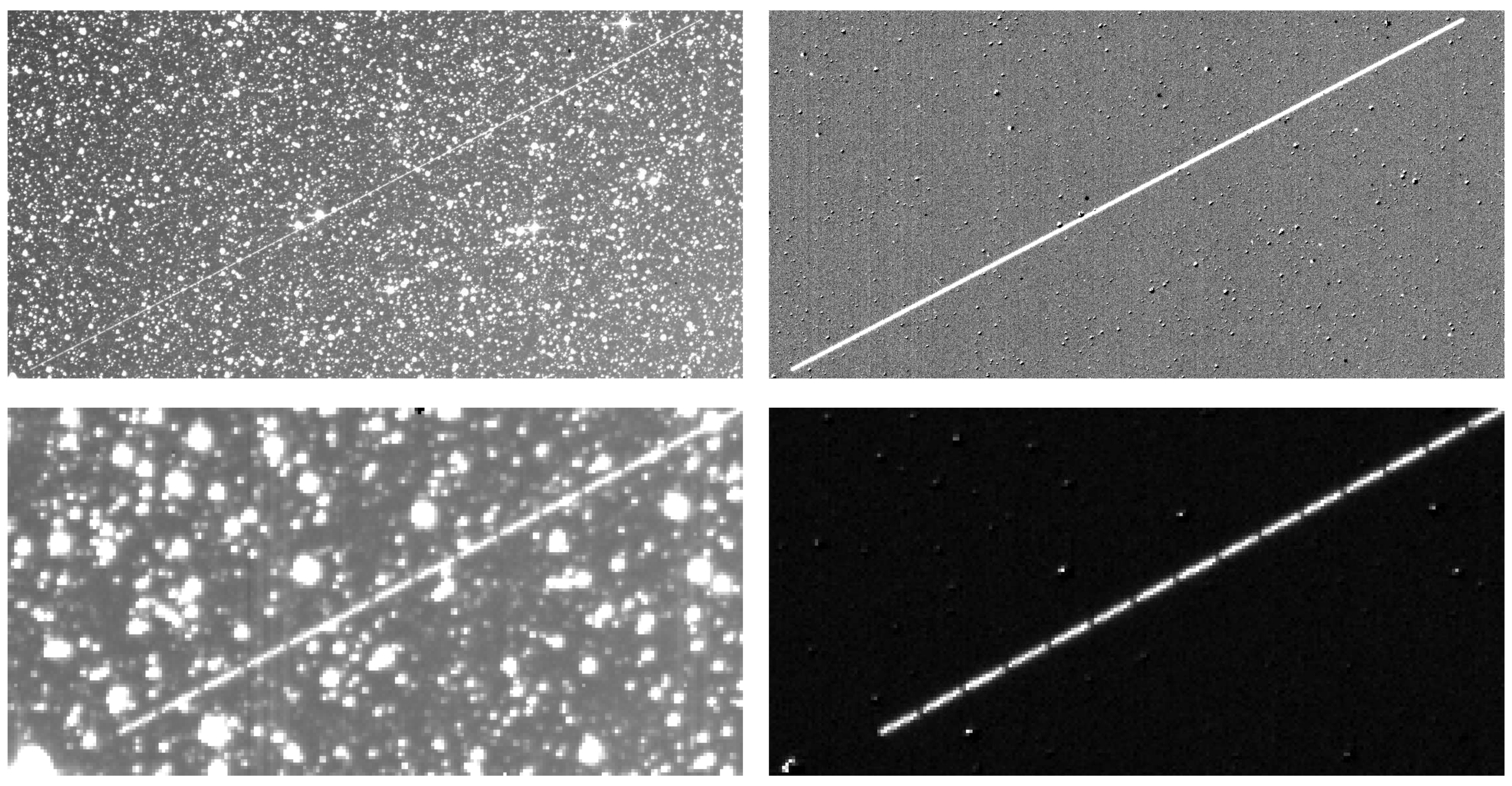

Fig. 1. *Upper left: The original 30-min exposure image corresponding to the cadence* `tess2019071195934-s0009-1-3-0139-s_ffic`*, showing the vicinity of the streak. The streak spans from* $(\alpha,\delta)=(11:50:02,-12:52.3)$ *to* $(11:23:18,-13:31.5)$*, i.e. it has a length of* $\sim 6^\circ.54$*. Upper right: The same field showing purely the streak. This differential image was computed by subtracting the median of the adjacent exposures (i.e. two images before and two images after the cadence of* `2019071195934`*). The good signal-to-noise ratio of the object is spectacular, implying a bright object. Lower left: A smaller section of the streak around* $(\alpha,\delta)=(11:50:02,-12:52.3)$*. The chopping due to the cosmic ray mitigation algorithm is visible. Lower right: The same section of the streak as in the lower left plot, shown on the differential image, but using a different scaling than on the image displayed on the upper right panel (namely, 99% percentage levels instead of the classic zscale algorithm). The chopping is quite prominent and unambiguous. One chopped section of the streak corresponds to the motion of the 20-second long elementary stacking unit of the TESS data acquisition cycle.*

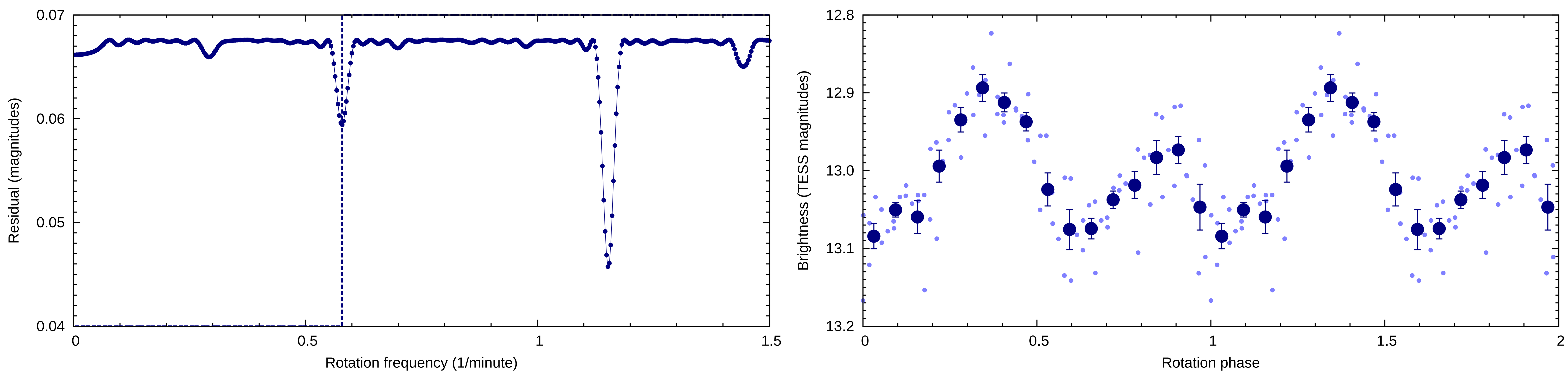

Fig. 2. *Left: The residual spectrum of the light curve of the object acquired on the image* `tess2019071195934-s0009-1-3-0139-s_ffic`*. The 30 minutes of gross exposure time corresponds well to the FWHM of the residual lines (which is* $0.0288\,\mathrm{min}^{-1}$*). Right: The folded light curve of this object, as folded with the frequency of* $n=0.5787\pm0.0063\,\mathrm{min}^{-1}$*. This frequency corresponds to the dashed line on the residual plot displayed on the left panel. Note that the clear double-peaked nature of this object yields the most prominent frequency at its double, at* $n_{\rm d}\approx 1.16\,\mathrm{min}^{-1}$*. The rotation period is then* $P=1.728\pm0.019,\mathrm{min}$*, indicating a small size below the spin-barrier limit. The overall brightness of this object is* $T\approx 13^{\rm mag}$*, Data processing has been performed using the tasks of the FITSH package [10], similar to [3].*

Summary and further work

The analysis of the streak of `tess2019071195934-s0009-1-3-0139-s_ffic` shows that:

- photometry can be performed with excellent accuracy, revealing the rotation characteristics (period, peak-to-peak amplitude) without any ambiguity;
- astrometry of the chopped parts can be derived with sub-arcsecond precision, $\lesssim 0.''5$ in this case;
- no known object could be associated to this streak → it is a discovery of something new which passes nearby, within one lunar distance; at this moment, unfortunately, we do not really know who it is and where it goes…

The progress of further work can be something like:

- implementation of a TESS-based orbit fit routine, providing initial orbital solutions;
- merging of data: this object above also appears in preceding and subsequent frames;
- some of the analysis steps can well be automatized; however, state-of-the-art software packages are not so suitable for analyzing these type of photographic features like chopped streaks;
- proper calibration of the magnitude zero point is essential: CMR could highly bias the apparent brightness since the 2-second long motion is comparable to the FWHM of the instrument PSFs.

References

[1] Pál, A., Molnár, L. & Kiss, Cs. 2018, PASP, 130, pp. 114503

[2] McNeill, A. et al. 2019, ApJS, 245, 29

[3] Pál, A. et al. 2020, ApJS, 247, 26

[4] Holman, M. J., Payne, M. J. & Pál, A. 2019, RNAAS, 3, 160

[5] Woods, D. F. et al. 2021, PASP, 133, id.014503

[6] Howell, S. B. et al. 2014, PASP, 126, 398

[7] Pál, A. et al. 2015, ApJ, 804, 45

[8] Vanderspek, R. et al. 2018 *TESS Instrument Handbook v0.1*, available from `https://heasarc.gsfc.nasa.gov/docs/tess/documentation.html`.

[9] Villaseñor, J. N. & Vanderspek, R. K. 2019, TESS Science Conference, poster presentation

[10] Pál, A. 2012, MNRAS, 421, 1825 (see also: `https://fitsh.net/`)